Materials Research Bulletin 46 (2011) 413–419

Contents lists available at ScienceDirect

Materials Research Bulletin

journal homepage: www.elsevier.com/locate/matresbu

Preparation of activated carbon from *sorghum pith* and its structural and electrochemical properties

S.T. Senthilkumar [a], B. Senthilkumar [a], S. Balaji [b], C. Sanjeeviraja [c], R. Kalai Selvan [a,*]

[a] Solid State Ionics and Energy Devices Laboratory, Department of Physics, Bharathiar University, Coimbatore 641046, India
[b] Materials Laboratory, Thiagarajar Advanced Research Center, Thiagarajar College of Engineering, Madurai 625015, India
[c] Department of Physics, Alagappa University, Karaikudi 630003, India

ARTICLE INFO

Article history:
Received 20 July 2010
Received in revised form 17 November 2010
Accepted 2 December 2010
Available online 9 December 2010

Keywords:
A. Amorphous materials
C. Electrochemical measurements
C. X-ray diffraction
D. Energy storage

ABSTRACT

The cost effective activated carbon (AC) has been prepared from sorghum pith by NaOH activation at various temperatures, including 300 °C (AC1), 400 °C (AC2) and 500 °C (AC3) for the electrodes in electric double layer capacitor (EDLC) applications. The amorphous nature of the samples has been observed from X-ray diffraction and Raman spectral studies. Subsequently, the surface functional groups, surface morphology, pore diameter and specific surface area have been identified through FT-IR, SEM, histogram and N_2 adsorption/desorption isotherm methods. The electrochemical characterization of AC electrodes has been examined using cyclic voltammetry technique in the potential range of −0.1–1.2 V in 1.0 M H_2SO_4 electrolyte at different scan rates (10, 20, 30, 40, 50 and 100 mV/s). The maximum specific capacitances of 320.6 F/g at 10 mV/s and 222.1 F/g at 100 mV/s have been obtained for AC3 electrode when compared with AC1 and AC2 electrodes. Based on the characterization studies, it has been inferred that the activated carbon prepared from sorghum pith may be one of the innovative carbon electrode materials for EDLC applications.

1. Introduction

Electric double-layer capacitors (EDLCs) are referred as supercapacitors or ultracapacitors [1]. EDLCs offer larger electrical energy storage capacity than the conventional capacitors due to their large interfacial area and the atomic range of charge separation (5–10 Å) between the electrode/electrolyte interfaces [2,3]. Supercapacitors have emerged as one of the promising energy storage systems due to their versatile properties like longer cycle life and higher power density than batteries and higher energy density than the conventional capacitors [4]. The carbon based materials such as activated carbon (AC), carbon nanotubes (CNTs), carbon aerogel, graphene and its composites are used as the electrodes for EDLC applications. Among these, activated carbon electrode is widely preferred [5] due its excellent properties such as easy processability, higher abundance, lower cost, inert to corrosion and higher endurance at high operating temperatures [6].

The specific capacitance of the activated carbons is dominated by several factors such as surface area, pore size distribution and surface functional groups [2]. The surface functional groups have a great impact on both electrostatic and non-electrostatic interactions [7] and the wettability of the electrodes [8]. The capacitance is mainly influenced by the pore size of the materials [9–13]. There are three different types of pore structures such as micro (<2 nm), meso (2–50 nm) and macro (>50 nm) pores [14]. Similarly wide ranges of literatures are available for the influence of surface area [12,15] and surface functional groups [10,16–18] on the specific capacitance of the super capacitors.

In general, capacitance is directly proportional to the specific surface area and hence the capacitance is expected to increase with the area as per the relation $C = \varepsilon_r\varepsilon_o A/d$, where '$\varepsilon_r$' is the electrolyte dielectric constant, 'ε_o' is the permittivity of a vacuum, 'A' is the specific surface area of the active material and 'd' is the effective thickness of the EDL. But this may not necessarily be valid for all carbon materials and it has already been proven by various research groups [6,15]. In their reports, they have insisted that the electrodes even with smaller surface area could yield large specific capacitance than those with large surface area. So, still now the relationship between pores (or) surface area and capacitance have not yet been clarified and this needs still more explorations through extensive research.

The pore structure and surface functional groups of the activated carbon can be controlled by various parameters, such as activation condition (activation agent, temperature and time) and nature of the precursors [7]. Especially for EDLC applications the activated carbons are mainly prepared by physical and chemical methods or the combination of both physicochemical methods [19] from many biomass materials such as waste

* Corresponding author. Tel.: +91 422 2428446; fax: +91 422 2425706.
E-mail address: selvankram@buc.edu.in (R. Kalai Selvan).

0025-5408/$ – see front matter © 2010 Elsevier Ltd. All rights reserved.
doi:10.1016/j.materresbull.2010.12.002

newspapers [20], seaweeds [21], cherry stones [22], coffee ground [23], corn grains [24], banana fibers [25], coffee shells [26] and sugar cane bagasse [27].

The main objective of the present work is to prepare activated carbon from agriculture waste product of sorghum pith through inexpensive physicochemical method. There are few literatures available on the preparation of activated carbon from grain sorghum for various applications [28,29] but to the best our knowledge no such reports exist on the preparation of activated carbon from sorghum pith for EDLC applications. The physico-chemical properties of the prepared activated carbons have been explored through various techniques like X-ray diffraction (XRD), Raman spectra, thermogravimetry analysis (TGA/DTA), scanning electron microscope (SEM), N_2 adsorption/desorption isotherm and Fourier transformer infrared spectroscopy (FT-IR). The electrochemical performance has been ascertained through cyclic voltammogram (CV).

2. Experimental

The sorghum pith was collected from nearby villages (Indur-Sirugaloor) of Dharmapuri District, Tamil Nadu (India). The AC was prepared by the following procedure. The dried sorghum pith in sunlight was fragmented into small pieces. These pieces were pyrolyzed at 200 °C for 12 h in vacuum and then, about 4 g of sample was activated in NaOH (20%) solution for 8 h. Further, these samples were carbonized in vertical tubular electric furnaces at various temperatures of 300 °C, 400 °C and 500 °C for 3 h in isolated atmosphere. The carbonized samples were washed by distilled water and least amount of HCl until the pH reaches ~7. The washed samples were dried at 200 °C for 24 h. The final product of activated carbons (ACs) are referred as AC1 (300 °C/3 h), AC2 (400 °C/3 h) and AC3 (500 °C/3 h). The XRD pattern was recorded on the powder sample of the activated carbons by using CuK_α radiation (30 mA, 40 kV, λ = 1.54 Å) (X'Pert PRO Diffractometer PANalytical) with the step size of 0.05° glancing angle and with the holding time of 10.14 s at fixed θ value at 25 °C. The natures of the ACs were explored through Raman spectroscopy (Horiba Jobin Raman spectrometer) analysis. The specific surface functional groups on the surface of the activated carbon samples was ascertained using FT-IR spectrometer (Nicolet Avatar Model FT-IR) in the range from 4000 cm^{-1} to 400 cm^{-1}. Thermal gravimetric analysis (TGA) was carried out using thermal analyzer (SDT Q600 V8.3 Build101) at a heating rate of 20 °C/min in air atmosphere. The surface morphologies of the samples were analyzed using scanning electron microscope (JSM-6390). The BET (Brunauer–Emmett–Teller) specific surface area (S_{BET}) of ACs was estimated from adsorption/desorption isotherms of N_2 at 77 K (ASAP 2020 V3.00 H) in this study.

The activated carbon electrodes were fabricated from the mixture of activated carbon (AC), polyvinylidene fluoride (PVDF) and graphite in the weight percent ratio 90:5:5 respectively. The above said mixture was made into slurry by dispersing in N-methyl 2-pyrrolidone and mixed slurry was coated over pretreated graphite strip with the area of 1 cm^2. Further the coated electrode was dried at 100 °C for few minutes and subjected to cyclic voltammetry.

The cyclic voltammetry was performed using (CHI 1120) with the above prepared carbon electrodes as working electrodes, Ag/AgCl electrode as the reference electrode and Pt wire as the counter electrode in 1.0 M H_2SO_4 electrolyte. The performance of the electrodes are tested in the potential ranging from −0.1 to 1.2 V at different scan rates viz., 10, 20, 30, 40, 50 and 100 mV s^{-1}. The specific capacitance of the AC electrode was calculated using Eq. (1) [30]:

$$C = \frac{i}{sm} \ (\mathrm{F/g}) \qquad (1)$$

where i, s and m are the average current, the scan rate and the weight of active material respectively.

3. Results and discussion

3.1. Thermal analysis

Fig. 1(a)–(c) shows the TGA/DTA curve of AC1, AC2 and AC3 samples. Generally, biomass consists of hemicelluloses, cellulose, lignin and extractives. Similarly, sorghum stem (pith is the major part of the stem) also consist of 20.5–29.9% of hemicelluloses, 25.8–31.7% of cellulose and 4.7–7.1% of lignin [31]. From Fig. 1, two different weight losses are observed within the measured temperature range from room temperature (RT) to 900 °C. The first weight loss has been observed around 100 °C for all the three samples and this may be due to the evaporation of volatiles that exist from dehydration of cellulosic structure or hemicelluloses and cellulose [19,27]. Since the lignin component mostly degrades at high temperature, the second weight loss occurred between 310 and 560 °C for all ACs has been attributed to the elimination of volatile component of lignin [19]. The obtained sharp DTA peaks at 486 °C (and 509 °C), 418 °C and 478 °C for samples AC1, AC2 and AC3 respectively indicate the exothermic phase transition associated with weight loss. The carbon content remaining in the biomass after combustion could be evaluated using the TGA curves [31–36]. As the sorghum pith biomass majorly constitutes hemicelluloses, cellulose and lignin content as sources for carbon,

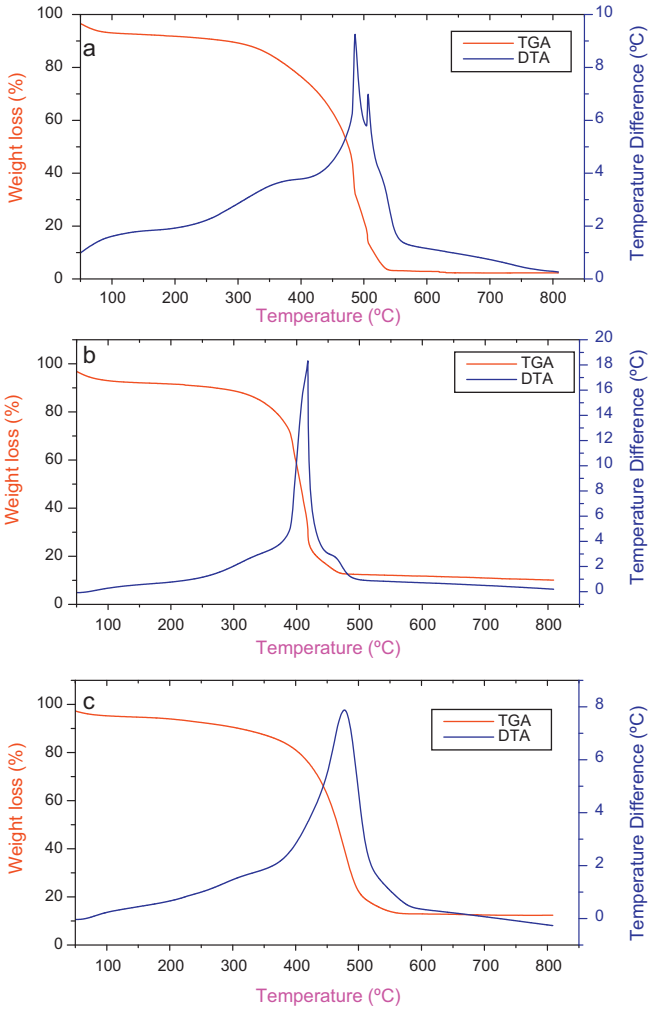

Fig. 1. TGA and DTA curve for (a) AC1, (b) AC2 and (c) AC3.

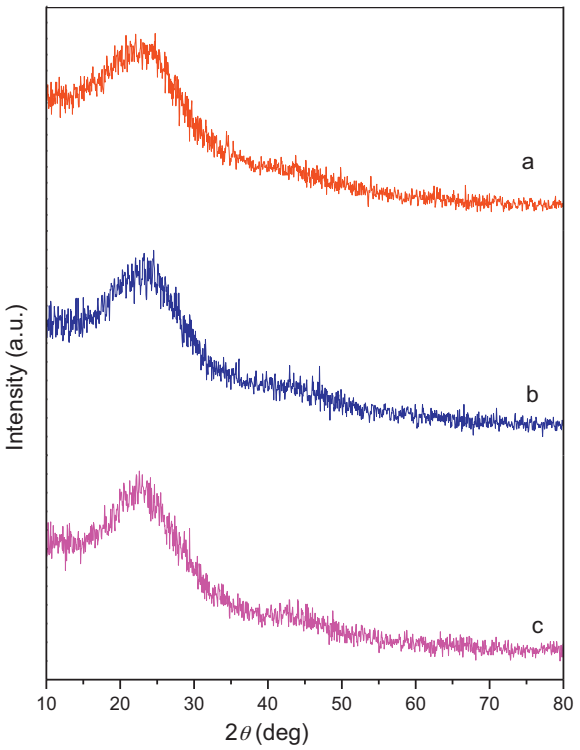

Fig. 2. The XRD pattern of (a) AC1, (b) AC2 and (c) AC3.

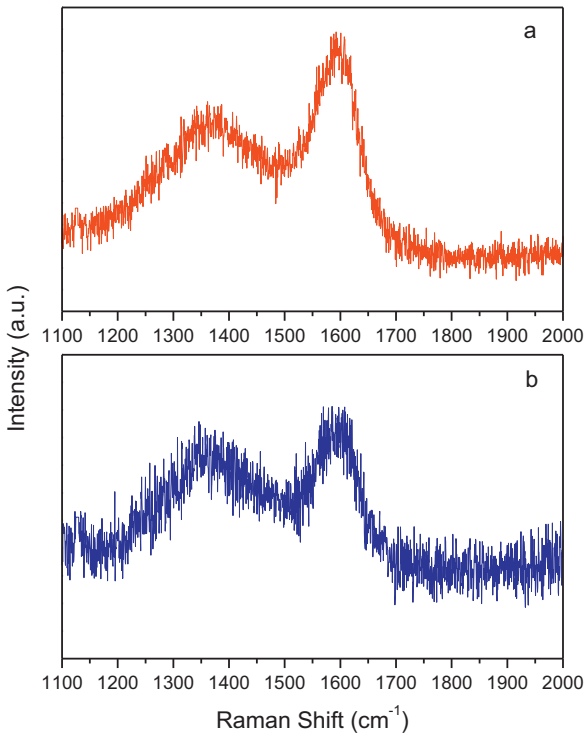

Fig. 3. Raman spectra of (a) AC1 and (b) AC3.

the mass remaining after the decomposition of lignin may be ascribed to the active carbon content. Thus approximately evaluated carbon contents in AC1, AC2 and AC3 are 43.85 wt%, 40.5 wt%, and 38.8 wt% respectively. The rest of the amount belongs to the moisture and volatile matter contents.

3.2. Structural analysis

The XRD patterns of the activated carbons (AC1, AC2 and AC3) are shown in Fig. 2. All the patterns show a strong peak between 23° and 30° which may be attributed to (0 0 2) diffraction peak, indicating the presence of amorphous nature and low graphitization. For the samples other than AC1, broad peak around 43° 2θ has been observed and this may be assigned to the (1 0) bidimensional planes as per Inagaki et al. The existence of *h k* (1 0) lines may be due to the turbostatic or convoluted stacking of hexagonal layers of carbon resulting in disordered structure and lower crystallinity [37,38]. The *R* factor values are also calculated for AC1, AC2 and AC3 and are provided in Table 1. According to Liu et al. [31], the empirical parameter *R* is defined as the ratio of the height of the (0 0 2) plane to the linear background. It is used to estimate the fraction of non-parallel single layers of carbon. From the table, it could be observed that the sample AC3 has low *R* value when compared with AC1 and AC2 samples. It indicates that AC3 contains more number of single layers due to the higher activation temperature and possess more amorphous characteristics and hence this sample is expected to yield better capacitance than rest of the samples [31,39].

In order to further investigate the nature of carbon, the materials were further subjected to Raman spectra. The representative Raman spectra of AC1 and AC3 are given in Fig. 3. It shows two broad peaks around 1360 cm^{-1} for disorder carbon structure (D-bond) and 1590 cm^{-1} for graphitic carbon (G-bond). The observed D- and G-bond could be attributed to the presence of A_{1g} Raman inactive and E_{2g} Raman active modes [40]. The calculated FWHM value of D- and G-bonds of AC3 is higher than that of other samples and this indicates the formation of more ordered amorphous or disordered carbon due to the higher activation temperature [41]. Furthermore, the calculated peak intensity ratio (I_D/I_G) of AC3 (0.97) is higher than that of AC1 (0.87). It also substantiates that the sample AC3 possess more amorphous nature than AC1 [40,41]. Thus the results from Raman spectra are well coinciding with the inference from XRD studies.

3.3. Morphology and surface area analysis

The SEM images of activate carbons (ACs) and corresponding pore size distribution histogram are shown in Fig. 4(a)–(f). It can be seen that the three SEM image shows the fibrous network with cavities or pores in different micron sizes. The cavities in ACs may be attributed to the evaporation of the activating agent which leaves space during carbonization as well as the subsequent

Table 1
Physical and electrochemical parameters.

Sample	2θ (°)	d_{002} (Å)	*R* factor	Pore size distribution (μm)	Pore size, D_{SCION} (μm)	Specific capacitance (F/g)	
						10 mV/s	100 mV/s
AC1	23	3.84	1.68	0.1–1.9	0.63	13.64	5.91
AC2	25	3.54	1.58	0.75–4.75	2.4	224.85	82
AC3	24	3.58	1.53	0.75–5.75	2.8	320.6	222

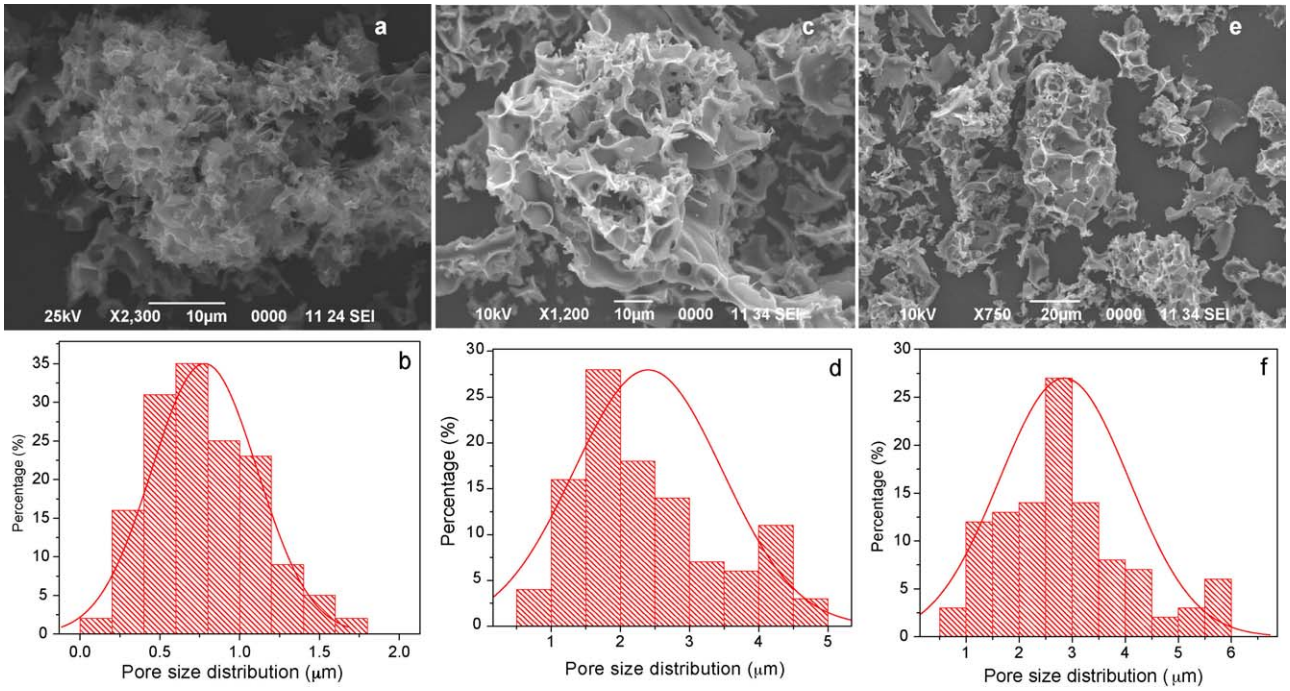

Fig. 4. SEM and pore size histogram of (a and b) AC1, (c and d) AC2 and (e and f) AC3.

removal of untreated NaOH by washing with water. The histogram gives the details about the average pore size (or) diameters and distributions. The average pore sizes of 0.63 μm, 2.4 μm and 2.8 μm are observed for AC1, AC2 and AC3 respectively. The similar range 3.9 and 5.9 μm of pore size has been reported by Kalpana et al. for activated carbon [20]. Similarly, the obtained pore size distributions are observed to be 0.1–1.9 μm for AC1, 0.75–4.75 μm for AC2 and 0.75–5.75 μm for AC3. From the above observations, it can be concluded that the pore size and pore size distributions increases with increase in the activation temperature. It may be due to the more elimination of volatile substances at higher temperature.

The estimated BET surface area values for corresponding ACs (AC1, AC2 and AC3), are observed to be 35 m^2/g, 27 m^2/g and 17 m^2/g via N_2 adsorption/desorption isotherms at 77 K. The observed surface area values are less when compared with the other activated carbons. Actually, the formation of high surface area in carbon materials is mainly based on the physical and chemical properties of the precursors and the processing parameters including activated conditions like temperature [42,43], activating agent [25,43] and ratio of activating agent/carbon [44] at different temperatures [22] and same temperature [45].

3.4. Functional groups analysis

FT-IR spectra of AC1, AC2 and AC3 are given in Fig. 5. The spectra of all activated carbons are complex due to the presence of many functional groups on their surface. The spectrum obtained for AC1 sample shows the characteristic peak at 3413.14 cm^{-1} corresponding to the O–H stretching vibration of the surface hydroxyl groups. This peak has been shifted to 3381.01 cm^{-1} for AC2 and 3419.25 cm^{-1} for AC3. The peak around 2921 cm^{-1} in all the samples endorses the presence of aliphatic C–H bond corresponding to the methylene group. A characteristic peak has been observed at 1599 cm^{-1} corresponding to C=O (carbonyl) stretching vibration in quinine or nitrogen quinine structure for AC1 sample and has undergone a shift to 1576 cm^{-1} and 1582 cm^{-1} for AC2 and AC3 samples respectively. In addition, the isolated –OH functional group is observed at 3730.46 cm^{-1} only for AC3 sample. On the other hand, characteristic peak at 763.21 cm^{-1} for AC1 and 759.07 cm^{-1} for AC2 samples corresponding to the bending mode of aromatic complex is observed. This vibration mode of aromatic complex is missing in the AC3 due to the higher activation temperature. From this study it could be inferred that the presence of carbonyl or quinine type groups on the surface (oxygen and

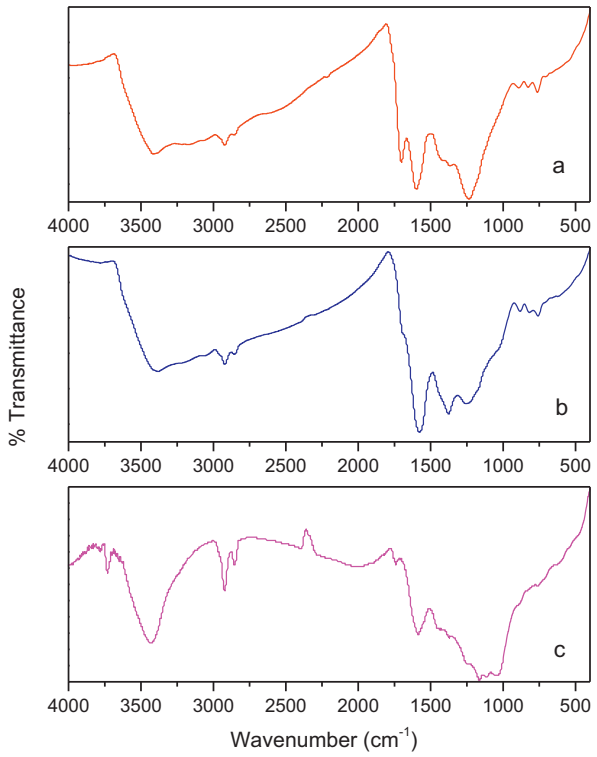

Fig. 5. FT-IR spectra of (a) AC1, (b) AC2 and (c) AC3.

nitrogen) of the activated carbon may influence the electrochemical performance of the electrodes [46,47]. Moreover, the quantity of other impurities has been observed to be insignificant to create an impact in the spectral studies and hence based on the spectral studies it could be corroborated that the carbonization of sorghum pith biomass may result in better quality carbon.

3.5. Electrochemical characterization

The capacitance behavior of activated carbon electrodes has been studied by CV in 1.0 M H_2SO_4 electrolytes with a potential window of −0.1–1.2 V vs. Ag/AgCl. Fig. 5(a)–(c) shows the cyclic voltammetric (CV) response of AC1, AC2 and AC3 electrodes performed at different scan rates of 10, 20, 30, 40, 50 and 100 mV/s. The specific capacitance values have been calculated using Eq. (1) and are given in Table 1. The shape of the CV curves for all the samples are more or less (quasi-) rectangular within the measured potential window and some redox peaks are also observed (Fig. 6). The observed redox peaks are due to the presence of trace amount of carbonyl group present in the surface of activated carbon. As a result of its existence an equilibrium reaction may occur on carbon electrodes as per Eq. (2) [46]:

$$>C_xO + H^+ \rightleftarrows >C_xO//H^+ \quad (2)$$

where $>C_xO//H^+$ denotes the proton adsorbed over the carbonyl group due to the induced ion-dipole attraction. As a result, the electric charge density gets changes, which leads making an excess specific double layer capacitance. During the charging of the negative electrode, the proton adsorbed over the carbonyl group can make a strong bond due to electron transfer across the double layer and vice versa for discharge process as per Eq. (3) [31]:

$$>C_xO + H^+ + e^- \rightleftarrows >C_xOH \quad (3)$$

This same behavior is discussed by Bleda-Martinez's groups [48]. This is the normal behavior which is well documented in the literature for various activated carbons [47,49,50]. At lowest scan rate of 10 mV/s, the measured specific capacitances are 13.64 F/g, 224.85 F/g and 320.6 F/g, for AC1, AC2 and AC3 respectively and a capacitance of 5.91 F/g, 82 F/g and 222.1 F/g, has been obtained at a higher scan rate of 100 mV/s for AC1, AC2 and AC3 respectively. Thus the specific capacity of AC3 sample is much higher than other samples. Moreover the observed specific capacitance values for AC3 is higher than the reported values of activated carbon prepared from other raw materials viz., the capacitance of 180 F/g at 2 mV/s for waste paper [20], 86 F/g at 5 mV/s for banana fibers [25] and 156 F/g at 1 mV/s for coffee shells [26] via CV curve. This observed higher capacitance may be due to the following reasons:

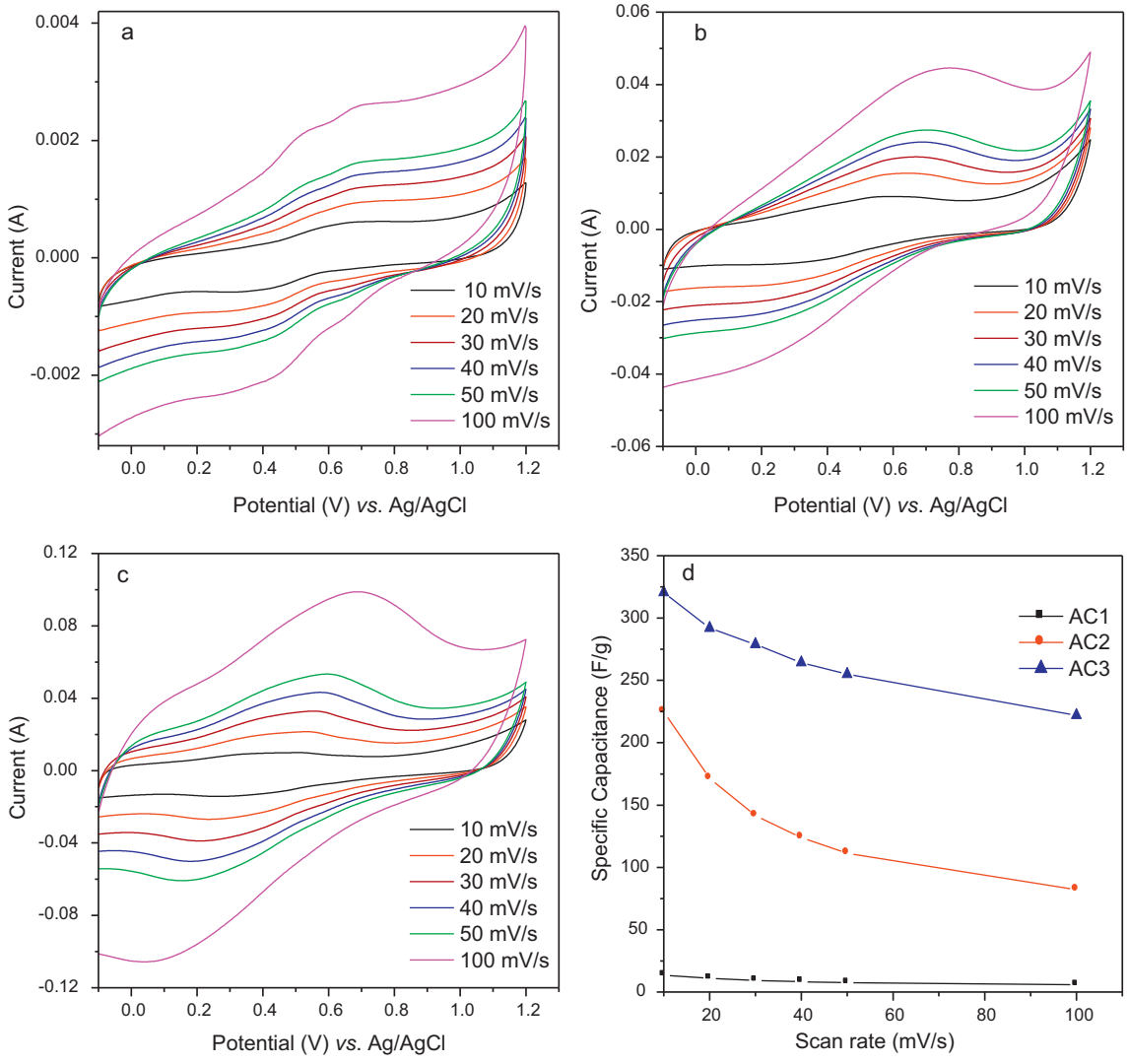

Fig. 6. CV curve of (a) AC1, (b) AC2 and (c) AC3 in 1 M H_2SO_4 electrolyte and (d) specific capacitance vs. scan rate of ACs.

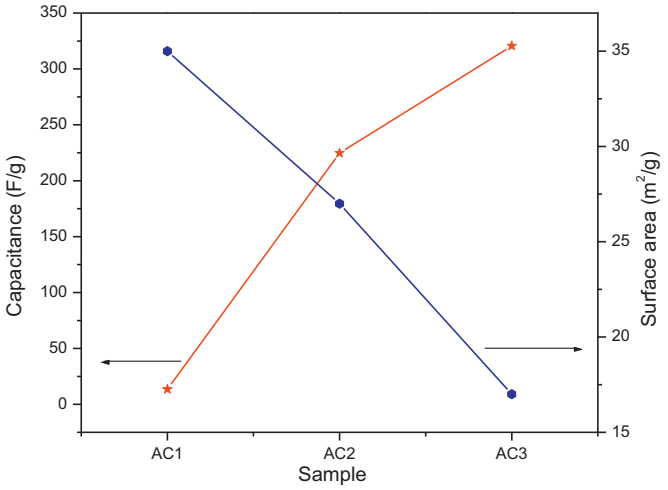

Fig. 7. Correlation between specific capacitance and specific surface area.

(i) the presence of additional isolated –OH functional group on the surface. The –OH groups may play a hydrophilic role to enhance wettability of ACs electrode and quick charge propagation. If the wettability of the electrode is high, formation of electrostatic double layer on the surface of electrode will be promoted and hence the associated capacitance adds up to the specific capacitance [51]. (ii) In the case of AC3 sample the pore size is higher than AC1 and AC2 (Table 1) which enhances the rate of adsorption of ions and in turn enhances the storage capacity. (iii) The low *R* factor value of AC3 has also got significant part in the capacity enhancement.

The current under curve has solely increased with increase in the scan rate, which indicates the dependence of voltammetric current on the scan rate. Fig. 6(d) shows the effect of specific capacitance with the scan rate of the two different activated carbon electrodes measured in the potential ranges of −0.1–1.2 V. It can be understood that the capacitance values decrease with the increase in scan rate. This is the common behavior of electrochemical systems. The extent of reduction in capacitance for AC3 sample from 320.6 F/g (10 mV/s) to 222.1 F/g (100 mV/s) is much higher when compared with other samples and this shows the extreme sensitivity of the electrode to scan rate.

The relationship between the specific capacitance and specific surface area of the samples is given in Fig. 7. It shows that the specific capacitance increases with activation temperature, whereas the specific surface area decreases. Generally, most of the literatures indicate that the surface area is an important parameter for observing higher specific capacitance. But in contrast, some of the researchers have reported and justified that the carbon materials having lower specific surface area can also give higher specific capacitance. Specifically, Lipka [52] has prepared carbon having very low surface area of 0.40, 0.35 and 0.70 m^2/g. Surprisingly, that carbon materials provided the high specific capacitance of 275 F/g (0.40 m^2/g), 310 F/g (0.35 m^2/g) and 190 F/g (0.70 m^2/g). Ironically, the higher surface area carbon material [42] has been observed to deliver the lower capacitance of 35 F/g (2694.5 m^2/g), 38.1 F/g (3089.2 m^2/g) and 40.8 F/g (2722.7 m^2/g). These results show that the specific capacitance depends not only upon the surface area, but also upon porosity, structure and surface functional groups of the carbon materials. Hence in this study, the effect of pore size and disorder has been observed to be predominant over the effect of specific surface area.

4. Conclusions

By employing physico-chemical method, activated carbon has been successfully prepared from sorghum pith by NaOH activation at different temperatures. The amorphous nature of the activated carbon has been confirmed from XRD and Raman spectra. The surface functional groups presented on the surface of activated carbon has been evaluated using FT-IR spectra. The pore size distribution, average pore size and BET specific surface area for all the samples have been elucidated from SEM images and N_2 adsorption/desorption isotherm analysis. The sample activated at 500 °C (AC3) gives the maximum specific capacitance of 320.6 F/g. Hence it could be concluded that the prepared activated carbon at high temperature (AC3) from sorghum pith would be one among the prominent electrode application for electric double-layer capacitors (EDLCs). Due to the adopted cost effective approach, it is strongly felt that the proposed activated carbon electrodes may witness burgeoning applications in the near future.

References

[1] A.G. Pandolfo, A.F. Hollenkamp, J. Power Sources 157 (2006) 11–27.
[2] L.L. Zhang, X.S. Zhao, Chem. Soc. Rev. 38 (2009) 2520–2531.
[3] Y. Zhang, H. Feng, X. Wu, L. Wang, A. Zhang, T. Xia, Int. J. Hydrogen Energy 34 (2009) 4889–4899.
[4] F. Lufrano, P. Staiti, Int. J. Electrochem. Sci. 4 (2009) 173–186.
[5] P. Simon, Y. Gogotsi, Nat. Mater. 7 (2008) 845–854.
[6] E. Frackowiak, F. Beguin, Carbon 39 (2001) 937–950.
[7] W. Shen, Z. Li, Y. Liu, Recent Patent Chem. Eng. 1 (2008) 27–40.
[8] D. Qu, J. Power Sources 109 (2002) 403–411.
[9] F.C. Wu, R.L. Tseng, C.C. Hu, C.C. Wang, J. Power Sources 144 (2005) 302–309.
[10] D. Lozano-Castello, D. Cazorla-Amoros, A. Linares-Solano, S. Shiraishi, H. Kurihara, A. Oya, Carbon 41 (2003) 1765–1775.
[11] J.A. Fernandez, S. Tennison, O. Kozynchenko, F. Rubiera, F. Stoeckli, T.A. Centeno, Carbon 47 (2009) 1598–1604.
[12] W. Li-Hong, M. Toyoda, M. Inagaki, New Carbon Mater. 23 (2008) 111–115.
[13] C. Vix-Guterl, E. Frackowiak, K. Jurewicz acrbon, M. Friebe, J. Parmentier, F. Beguin, Carbon 43 (2005) 1293–1302.
[14] M. Inagaki, New Carbon Mater. 24 (2009) 193–232.
[15] O. Barbieri, M. Hahn, A. Herzog, R. Kotz, Carbon 43 (2005) 1303–1310.
[16] M.J. Bleda-Martinez, D. Lozano-Castello, E. Morallon, D. Cazorla-amoros, A. Linares-Solano, Carbon 44 (2006) 2642–2651.
[17] M.J. Bleda-Martine, J.A. Macia-Agallo, D. Lozano-Castello, E. Morallon, Carbon 43 (2005) 2677–2684.
[18] M. Seredych, D. Hulicova-Jurcakova, G.O. Lu, T.J. Bandosz, Carbon 46 (2008) 1475–1488.
[19] V. Sricharoenchaikul, C. Pechyen, D. Aht-ong, D. Atong, Energy Fuels 22 (2008) 31–37.
[20] D. Kalpana, S.H. Cho, S.B. Lee, Y.S. Lee, R. Misra, N.G. Renganathan, J. Power Sources 190 (2009) 587–591.
[21] E. Raymundo-Pinero, M. Cadek, F. Beguin, Adv. Funct. Mater. 19 (2009) 1032–1039.
[22] M. Olivares-Marin, J.A. Fernandez, M.J. Lazaro, C. Fernandez-Gonzalez, A. Macias-Garcia, T.A. Centeno, Mater. Chem. Phys. 114 (2009) 323–327.
[23] T.F. Rufford, D.H. JurcaKova, E. Fiset, Z. Zhu, G. Qing Lu, Electrochem. Commun. 11 (2009) 974–977.
[24] M.S. Balathanigaimani, W.G. Shim, M.J. Lee, C. Kim, J.W. Lee, H. Moon, Electrochem. Commun. 10 (2008) 868–871.
[25] V. Subramanian, C. Luo, A.M. Stepen, K.S. Nahm, S. Thomas, B. Wei, J. Phys. Chem. C 111 (2007) 7527–7531.
[26] M.R. Jisha, Y.J. Hwang, J.S. Shin, K.S. Nahm, T.P. Kumar, Mater. Chem. Phys. 115 (2009) 33–39.
[27] T.E. Rufford, D.H. Jurcakova, K. Khosla, Z. Zhu, G. Qing Lu, J. Power Sources 195 (2010) 912–918.
[28] Y. Diao, W.P. Walawender, L.T. Fan, Bioresour. Technol. 81 (2002) 45–52.
[29] H. Bapat, S.E. Manahan, D.W. Larsen, Chemosphere 39 (1999) 23–32.
[30] R. Kalai Selvan, I. Perelshtein, N. Perkas, A. Gedanken, J. Phys. Chem. C 112 (2008) 1825–1830.
[31] Y. Liu, J.S. Xue, T. Zheng, Carbon 34 (1996) 193–200.
[32] S.H. Ng, J. Wang, D. Wexler, S.Y. Chew, H.K. Liu, J. Phys. Chem. C 111 (2007) 11131–11138.
[33] Z. Yue, J. Economy, K. Rajagopalan, G. Bordson, M. Piwoni, L. Ding, V.L. Snoeyinkc, B.J. Marinas, J. Mater. Chem. 16 (2006) 3375–3380.
[34] S.L. Chou, J.Z. Wang, C. Zhong, M.M. Rahman, H.K. Liu, S.X. Dou, Electrochim. Acta 54 (2009) 7519–7524.
[35] M.M. Rahman, S.L. Chou, C. Zhong, J.Z. Wang, D. Wexler, H.K. Liu, Solid State Ionics 180 (2010) 1646–1651.
[36] T. Yuan, X. Yu, R. Cai, Y. Zhou, Z. Shao, J. Power Sources 195 (2010) 4997–5004.
[37] G.Q. Zhang, S.T. Zhang, J. Solid State Electrochem. 13 (2009) 887–893.
[38] B. Viswanathan, P.I. Neel, T.K. Varadarajan, Method of Activation and Specific Application of Carbon Materials, 2009 February.
[39] N. Shimodaira, A. Masui, J. Appl. Phys. 92 (2002) 902–909.
[40] A. Janes, H. Kurig, E. Lust, Carbon 45 (2007) 1226–1233.
[41] D. She, F. Xu, Z. Geng, R. Sun, R. Sun, G.L. Jones, M.S. Baird, Ind. Crop. Prod. 32 (2010) 21–28.

[42] X.Y. Zhao, J.P. Cao, K. Morishita, J.I. Ozaki, T. Takarada, Energy Fuels 24 (2010) 1889–1893.
[43] S. Roldan, I. Villar, V. Ruiz, C. Blanco, M. Granda, R. Menendez, R. Santamaria, Energy Fuels 24 (2010) 3422–3428.
[44] M.J. Bleda-Martinze, D. Lozano-Castello, D. Cazorla-Amoros, E. Morallon, Energy Fuels 24 (2010) 3378–3384.
[45] D. Hulicova, J. Yamashita, Y. Soneda, H. Hatori, M. Kodama, Chem. Mater. 17 (2005) 1241–1247.
[46] C.T. Hsieh, H. Teng, Carbon 40 (2002) 667–674.
[47] E. Frackowiak, Phys. Chem. Chem. Phys. 9 (2007) 1774–1785.
[48] M.J. Bleda-Martine, D. Lozano-Castello, E. Morallon, D. Cazorla-Amoros, Carbon 43 (2005) 2677–2684.
[49] W. Li, D. Chen, Z. Li, Y. Shi, Y. Wan, Electrochem. Commun. 9 (2007) 569–573.
[50] M. Kang Seo, S. Yang, I.J. Kim, Mater. Res. Bull. 45 (2000) 10–14.
[51] B. Fang, L. Binder, Electrochim. Acta 52 (2007) 6916–6921.
[52] T. Lipka, IEEE AES Syst. Mag. July (1997) 27–30.